

Sensitivity analysis of finger-vein recognition models

Dalibor Maljurič¹, Klemen Grm^{†1}

¹ *Machine Intelligence Lab, Faculty of Electrical Engineering, University of Ljubljana, Tržaška 25, 1000 Ljubljana, Slovenia*

[†] *E-mail: klemen.grm@fe.uni-lj.si*

Abstract. Finger vein recognition has gained a lot of attention in recent years due to the high robustness of existing recognition models against spoofing attacks as well as their high recognition performance. A lot of effort has been put into improving the performance of the recognition models over the years while studies exploring their robustness have not received a comparable amount of attention in the literature. The paper tries to fill this gap by empirically analysing the robustness of three popular finger vein recognition models, i.e., *Repeated Line Tracking* (RLT), *Maximum Curvature* (MC), and *Wide Line Detector* (WLD), against four types of image distortions, i.e., blur, two types of noise and JPEG2000 compression, and evaluating their impact on the verification performance of the three selected models. Experimental results on the VERA finger vein dataset show that the tested finger vein models are highly susceptible to the presence of noise and blur, whereas compression artifacts have only a limited affect on the overall recognition performance.

Keywords: Biometrics, deep learning, vein recognition

Analiza občutljivosti modelov za razpoznavanje žil

Področje razpoznavanja žil je bilo v zadnjih letih deležno veliko pozornosti zaradi modelov, sposobnih robustnega delovanja pri razpoznavanju žil kljub prisotnosti prevarantskih napadov. Veliko napredka je bilo narejenega na področju izboljšave delovanja modelov razpoznavanja, manj pa študij o robustnosti teh modelov. V tem članku poskušamo zapolniti to vrzel preko kvantitativnega vrednotenja robustnosti treh izmed najbolj uporabljenih modelov za razpoznavanje žil, *Repeated Line Tracking* (RLT), *Maximum Curvature* (MC), and *Wide Line Detector* (WLD), ob prisotnosti štirih različnih virov popačenja slik - glajenja, Gaussovega šuma, šuma "sol in paper", ter kompresije z algoritmom JPEG2000. Za vsak vir popačenja slik sistematično ovrednotimo delovanje omenjenih modelov za razpoznavanje žil. Rezultati na podatkovni zbirki Vera finger vein dataset kažejo, da so izbrani modeli močno občutljivi na šum in glajenje, kompresijski artefakti pa imajo manjši vpliv na uspešnost razpoznavanja.

Ključne besede: biometrija, globoko učenje, razpoznavanje žil.

1 INTRODUCTION

Finger vein recognition has received a considerable amount of attention over recent years. The interest in the technology is fueled by the performance of existing recognition models and more importantly by the resilience of finger vein recognition techniques to spoofing attacks [1], [2], [3], [4], [5]. While a lot of

work has been done over the years to improve recognition performance in this area, considerably less effort has been put into studying the robustness of existing recognition models. Recognition techniques are typically tested on standard finger vein datasets with high-quality images without obvious image degradations such as high levels of noise, blur or compression artifacts, which can easily be present in real world applications due to detector errors, finger movement, storage constraints, image transmission, and other external circumstances.

Research on the robustness of finger vein models is heavily underrepresented in the literature, which is an issue given the fact that understanding the strengths and weaknesses of the existing models is of paramount importance to their robustness in real-life deployment scenarios. While there have been prior efforts taken to investigate the robustness of finger vein models [6], [7], [8], they have been limited to a handful of image distortions (e.g., compression or longitudinal finger rotation) or evaluating models on different databases with images of varying quality [9]. To the best of our knowledge, there has been little to no work done in terms of a comprehensive study of robustness of finger vein models that would consider multiple image distortions in a common evaluation framework.

When assessing the robustness of a finger vein model, distortions are typically added to the input images and an analysis is conducted on how the strength of the added distortion affects the performance of the model. Images are usually distorted in a manner corresponding

to real-world environments, where image capture errors can occur or compression is applied to the images due to storage constraints. In [6], [7], an analysis is then performed to determine how image distortions affect the recognition accuracy of the finger vein model considered.

The paper follows this general methodology and explores the strengths and weaknesses of finger vein models through a comprehensive study of the robustness of the models against different types and levels of image distortion. The paper analyzes the affects of multiple types of image distortions on the verification accuracy of three finger vein models for which an open source implementation is available online. We use the Repeated Line Tracking (RLT) [4] model, the Maximum Curvature (MC) [3] model, and the Wide Line Detector (WLD) [1] model to extract vein features from the input images. We then use the features to explore how different types of image distortion such as noise, blur and compression artifacts affect their accuracy. The accuracy of the tested models is evaluated on the VERA finger vein database [9], which is regarded as a challenging database in terms of preprocessing, alignment and recognition. Our study suggests that the performance of the tested finger vein models is decreased substantially when different sources of image degradation are present at the input.

Compared to existing robustness studies involving finger vein recognition models, our two main contributions are:

- We conduct a comprehensive analysis of the robustness of three popular finger vein models and investigate the impact of multiple types of image degradations (i.e., two types of noise, blur and compression artifacts) on their performance using a consistent evaluation framework.
- We contribute towards a better understanding of existing finger vein recognition models and make novel findings not reported in the literature before.

2 RELATED WORK

This section provides a brief review existing work relevant to our analysis. We first present an overview of existing finger vein recognition methods and then summarize prior work related to the robustness of existing models in the field of finger vein recognition. The reader is referred to [10] for a comprehensive coverage of the topic of finger vein recognition.

2.1 Finger vein models

A significant amount of work in the field of finger vein recognition focuses on the feature extraction stage, which is crucial for achieving high recognition performance. Among existing methods from this group the , Repeated Line Tracking (RLT) and Maximum Curvature

(MC) approaches of Miura *et al.* [4], [3] are particularly popular in the research community and used also in existing robustness studies [6], [7]. The RLT approach [4] extracts finger-vein patterns by using line tracking that starts from various positions, whereas the MC technique from [3] determines local maximum curvatures of cross-sectional profiles of veins and extracts consistent center-lines that are unaffected by variations in the vein width and brightness. Another standard finger vein extraction technique often used in the literature is the Wide Line Detector (WLD) [1]. Here, the authors propose a wide line detector for feature extraction and a new pattern normalization model which can effectively reduce the distortion caused by finger pose.

Among the more popular feature extraction techniques for finger vein recognition are methods based on Gabor filtering, which excel at extracting texture characteristics. In [11], the authors combined the Weber Local Descriptor (WLD) with curvature Gabor filters for finger vein recognition. In [5] the authors applied convolutional neural networks (CNNs) to learn the parameters of a bank of Gabor filters automatically and report promising results.

Another popular feature extraction technique for finger vein recognition is Local Binary Patterns (LBP). An example of work based on LBP is presented by Xiong *et al.* [12]. Here, the authors improve on the classic LBP technique by adopting a center-symmetric local binary patterns (CSLBP), that reduce feature dimensions and provide better robustness to noise. Another study based on LBP is described by Hu *et al.* [13]. Here, the authors combine the LBP operator with 2D-PCA for feature compression and again achieved competitive recognition performance.

With the recent advancements in deep learning, attempts have been made to incorporate Deep Neural Networks (DNNs) into finger vein recognition models. An example of a deep learning implementation of finger vein recognition was proposed in [14]. Specifically, the authors present a combination of canonical correlation analysis (CCA) and PCANet as a new filter generation method and report results comparable to state-of-the-art models. In [15], the authors also use a CNN-based model to learn finger vein features that are more discriminative and robust than handcrafted features. They demonstrated that their end-to-end method can address the problem of misalignment caused by translations and rotations in finger vein images to a certain degree.

We select the RLT, MC and WLD feature extraction techniques which are standard finger vein feature extraction techniques used for analysis of finger vein models. Our choice is motivated by the popularity of the three techniques, their performance with respect to the state-of-the-art and the fact that open-source implementations are readily available and contribute to the reproducibility

of our analysis.

2.2 Performance assessments of the finger vein models

There has been a considerable amount of done in the past few years to develop new models for finger vein recognition. In contrast, studies of the robustness of these models are still limited in the literature, despite their importance for practical deployment aspects.

An example of work studying the impact of image degradation on finger vein recognition was presented by Ablinger *et al.* [6]. The authors explore the effects of different compression standards on finger vein recognition accuracy. They conclude that images can be compressed heavily while still enabling competitive finger vein recognition performance due to the large uniform areas present in these images.

Another study presented by Prommegger *et al.* [7] explores the influence of longitudinal rotation on the performance of finger vein recognition systems, and the degree to which adverse effects can be circumvented. The authors confirm the adverse impact of longitudinal rotation on the recognition performance of finger vein models and show that its correction noticeably improves performance.

In [8] the authors presented a more comprehensive analysis of a finger-vein based biometric identification system on four publicly available databases to assess the effectiveness of the proposed network under different image quality conditions. But unlike the research in [6] no image quality related covariate was found to significantly affect performance.

All of the above studies have had a profound impact on the development of finger vein recognition technology by providing valuable information on the weaknesses of finger vein models in non-ideal conditions commonly encountered in real-world biometrics applications. In this work, we further contribute to a better understanding of the robustness of standard finger vein models to image degradations by comprehensively studying different types of image distortions at various intensity levels.

3 METHODOLOGY

In this section we present the methodology used to assess the robustness of three finger vein models. We first introduce the dataset adopted to perform model evaluations and then present the methodology defined for the experiments. Next, we elaborate on the finger vein models selected for the analysis and finally describe the distortions considered in this work.

3.1 The VERA Finger vein Database

The VERA Finger Vein database [9], collected at the Idiap Research Institute, consists of 440 images from

110 subjects and contains images of both index fingers of all subjects, i.e., 2 images per finger. 40 of the subjects are women and 70 are men. Subject age ranges between 18 and 60 years, with an average of 33 years. Images were acquired in one session with 2 images per finger, with a 5 minute separation between the acquisitions. The recording was performed at 2 different locations, always inside buildings with normal light conditions. All of the 440 images are stored in PNG format with a resolution of 250×665 pixels. The database also contains extracted ROI images with a resolution of 150×565 pixels. The database was chosen because it is one of the standard finger vein databases and one of the more challenging databases regarding recognition. For the purposes of our evaluation, we use the full resolution images. For the experiments, we resize all images using a scale factor of 0.4 and then apply the finger localisation method from [16] to mask out background pixels (i.e. by setting them to 0). The final resolution of the images is 100×266 pixels.

3.2 Evaluation Methodology

To study the robustness of finger vein models with respect to different types of image distortions, we select three finger vein models for analysis and assess their performance in a verification experiment. The output for each of the models is a vein image (referred to as *feature image* hereafter) of the same dimensions as the input image. This transformation can be described as a mapping of the following form: $y = f(x)$, where $x \in \mathbb{R}^{n \times m}$ is the input image, $f(\cdot)$ represents the selected finger vein model and $y \in \mathbb{R}^{n \times m}$ is the generated feature image. When the feature images are computed (see Fig. 1), we calculate a similarity score R_M between each image pair. Based on the similarity score, the matching decision function τ is:

$$\tau(x_1, x_2, f, \Delta) = \begin{cases} w_1, & \text{if } R_M(y_1, y_2) \geq \Delta \\ w_2, & \text{otherwise,} \end{cases} \quad (1)$$

where x_1 and x_2 are the input images to be matched, $R_M(\cdot, \cdot)$ is the Miura score [3], Δ is a chosen decision threshold and w_1 and w_2 are class labels corresponding to matching and non-matching verification attempts, respectively. For a given pair of input images the decision function should assign class label w_1 when the identities of the fingers match and class label w_2 when the identities do not match. To study the robustness of the considered finger vein models, their accuracy is first determined without altering the input images x_1 and x_2 in Eq.(1). This serves as a reference for all considered finger vein models and represents the basis for evaluating the impact of image distortions. In all experiments image distortions are added to one of the input images, while leaving the second image unaltered. By adopting such a setup, one can directly observe the

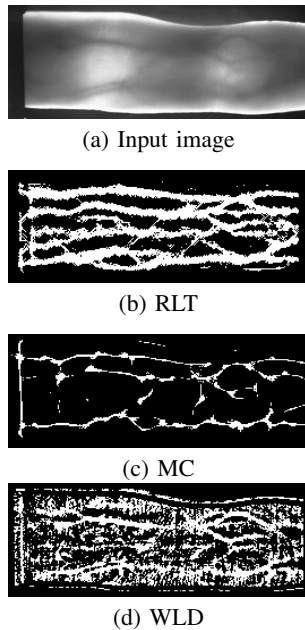


Figure 1.: Visual examples of the feature images generated by the three finger vein models selected for the analysis in this paper. The figure shows: (a) the original grey-scale input image, and feature images generated by (b) the RLT, (c) the MC and (d) the WLD finger vein models.

change in model verification accuracy due to the quality miss-match between the two images being compared.

3.3 Feature extraction techniques

For the finger vein models, three feature extraction techniques are chosen, for which an open source implementation is publicly available online. Each feature extraction technique returns a binary vein image that is of the same dimensions as the input image. Examples of the feature images generated by the three models are shown in Fig. 1. Note the difference in the appearance of the feature images. Below we describe the selected models in more detail:

- *Repeated Line Tracking (RLT)* [4] takes advantage of the fact that veins appear as valleys in the cross-sectional profile of the input images. A randomly initialised tracking point is moved pixel by pixel along a dark line that corresponds to a valley and the depth of the valley indicates the movement direction. If no valley is detected, a new tracking operation is started. The number of times a pixel is tracked is recorded in a matrix, called locus space. Pixels that are tracked multiple times have a high likelihood of belonging to a blood vessel (high value in the locus space image). Binarization is, therefore, applied to the locus space image to get the final binary output image. An example of the binary feature image generated by the RLT model

is shown in Fig. 1(b).

- *Maximum Curvature (MC)* [4] emphasises the center lines of the veins and is therefore insensitive to changes in the width of the veins. The first step of this model is the extraction of the center positions of the veins. For this purpose, the local maximum curvature in cross-sectional profiles in four directions, i.e., horizontal, vertical and the two oblique directions, is determined based on the first- and second-order derivatives. Then, each profile is classified as being concave or convex (curvature positive or negative), where local maxima in concave profiles indicate the center positions of the veins. Finally, each center position is assigned a score according to the width and curvature of the region. An example of a feature image generated by the MC feature extraction technique is presented in Fig. 1(c).
- *Wide Line Detector (WLD)* [1] works similarly to the adaptive thresholding (using isotropic nonlinear filtering) and relies on thresholding inside a local neighbourhood region. Here, the difference between each pixel inside a circular neighbourhood and the central pixel of the neighborhood is calculated first. If the difference exceeded a predefined threshold, the pixel is set to 0, if not, the pixel is set to 1. The procedure returns a binary feature image with vein patterns clearly visible in the output (Fig. 1(d)).

3.4 Distortion Sources

To study the effect of image degradation on the performance of finger vein models, we consider three sources of image distortion, i.e., noise, blur and image compression.

We use Gaussian blur to simulate sources of blur such as motion or sensor distortions. We use noise as a simulation of sensor and circuitry problems during image capture. Finally, we also study compression artifacts as they are a common problem arising from low-bandwidth communications. Each of image distortion represents problems that can be encountered in real-life biometric applications. We apply the distortions separately with different levels to the probe images x and then process the distorted images \hat{x} with the finger vein models described in the previous section, or formally:

$$\hat{x} = \delta(x, \theta), \quad (2)$$

where \hat{x} is the degraded finger vein image, $\delta(\cdot)$ is a distortion function and θ are the parameters of the distortion function that determine the extent of the distortion. Below we describe the image distortions δ considered in this work in more detail:

- *Gaussian noise*: The first distortion considered in the experiments is additive Gaussian noise with

mean $\mu = 0$ and varying standard deviation σ , thus, $\theta = \{\mu, \sigma\}$. Gaussian noise is added to a finger vein image using the following operation:

$$\hat{x} = \max(0, \min(255, x + g)), \quad (3)$$

where $x \in \mathbb{R}^{n \times m}$ is the input image, $g \in \mathbb{R}^{n \times m}$ represents random Gaussian noise drawn from $\mathcal{N}(0, \sigma)$, and $\hat{x} \in \mathbb{R}^{n \times m}$ is the corrupted output image. For the analysis, we let σ vary from 10 to 100 in steps of 10.

- *Salt-and-pepper noise*: The second distortion studied in the experiment is salt-and-pepper noise. Here, we set the pixel values of the finger vein image either to 0 or 255 with a probability of $\rho/2$ each (thus, $\theta = \{\rho\}$). For the experiment, we generate 10 modified probe sets corresponding to probabilities ρ between 0.05 and 0.5, sampled uniformly with a step size of 0.05.
- *Blur*: The next distortion we consider is blurring. To this end, we take a Gaussian kernel and vary the standard deviation of the kernel from 1 to 10 in steps of 1. We implement blurring via the discrete convolution using square kernels of size $2\lceil 2\sigma \rceil + 1$, where $\lceil \cdot \rceil$ is the ceiling operator. The parameters of this distortion function are defined by the standard deviation of the blurring kernel, i.e., $\theta = \{\sigma\}$.
- *JPEG2000*: The last distortion we consider is JPEG2000 compression. We subject the original images to varying degrees of compression and observe the impact on verification performance. The level of compression is measured with a compression ratio ζ , i.e., the ratio of the original file size and the compressed file size. For our experiments, we let the compression ratio ζ vary from 20 to 200 in steps of 20, i.e., $\theta = \{\zeta\}$.

In Fig. 2 we show some examples of images degraded with different distortion functions and levels of distortions.

4 EXPERIMENTAL RESULTS

In this section we discuss the experimental setup, performance metrics and the results of our sensitivity analysis.

4.1 Experiment Setup

The open source finger vein framework PLUS OpenVein Toolkit is used for the experiments. The toolkit implements a full feature extraction and matching/evaluation framework for finger- and hand- vein recognition in MATLAB.

For the evaluation, we use the test procedure defined by the Vera Full protocol [9]:

- We use the first image of both index fingers (of all 110 subjects) for the enrollment. This results in 220 unique fingers (or classes) and corresponds to 220 distinct images.

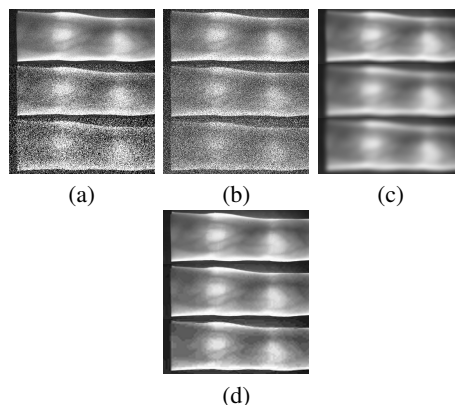


Figure 2.: Visual examples of the image degradations caused by the distortion functions considered in this paper at varying levels of intensity. From left to right: (a) Gaussian noise with different σ (top to bottom): 10, 50, 100, (b) salt and pepper noise with different levels of ρ (top to bottom): 0.1, 0.3, 0.5, (c) Gaussian blur with different σ levels (top to bottom): 3, 5, 10. and (d) compression artifacts with different compression ratios ζ (top to bottom): 50, 100, 200.

- We compare the second image (i.e., the probe) of all classes with the corresponding enrollment image. This amounts to 110 genuine scores.
- We compare the probe image of a given class with the enrollment images of all the other classes. Thus, we compute a total of 11990 impostor scores

Both the genuine and impostor scores are obtained with the matching method proposed in [3], which is a similarity measure based on correlation.

4.2 Performance Metric

To evaluate the performance of the finger vein recognition models, we report equal error rates (EER) for all experiments. The EER metric was chosen because it is a standard metric for evaluating biometric verification systems [17]. The equal error rate is defined as the operating point on the Received Operating Characteristics (ROC) curve, where the false acceptance rate (FAR) and false rejection rate (FRR) are equal. Lower EERs corresponds to better verification performance.

4.3 Baseline Performance

To observe the effect of each distortions on the verification accuracy of the tested models, we first report the reference EER values computed on the original (undistorted) images in Table 1. The MC model achieves the highest verification accuracy (lowest EER) on the VERA database. Compared to RLT and WLD, the MC model achieves half the EER score. These results are somewhat higher compared to the results reported in similar studies where the same models were evaluated on different databases [6]. This can be partially contributed

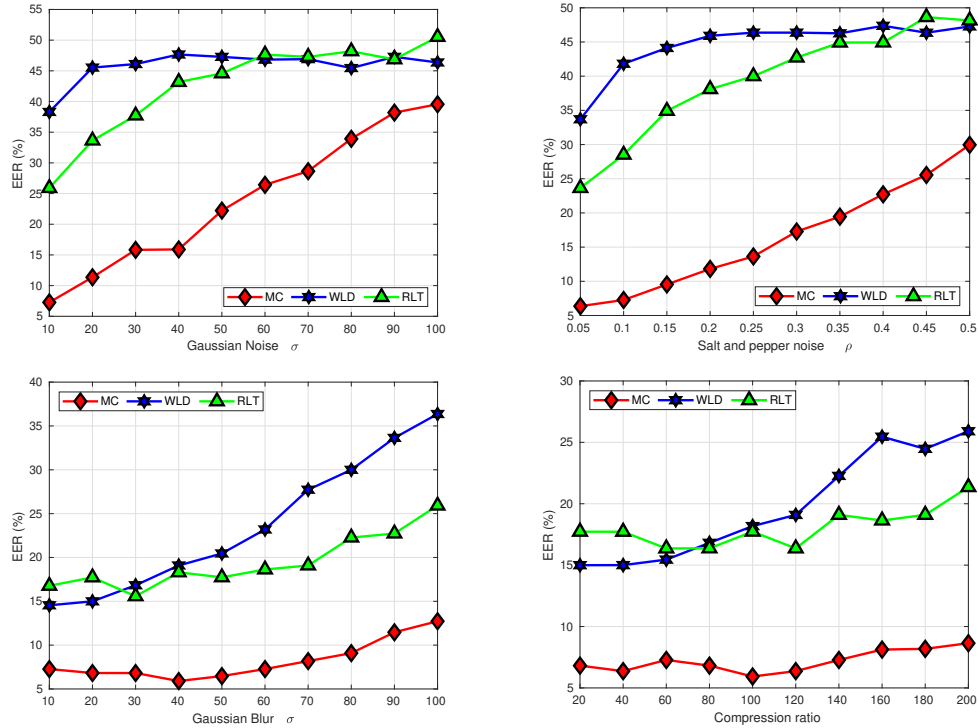


Figure 3.: Impact of different sources of image degradations on the verification accuracy of three finger vein models measured in terms of EER: (left to right and top to bottom): Gaussian noise, salt-and-pepper noise, Gaussian blur, compression artifacts.

Table 1.: Reference EER values for the three models obtained on the original (undistorted) images.

Model	MC	RLT	WLD
EER [in %]	7.26	18.17	14.99

to the more challenging nature of the finger vein images in the VERA database.

4.4 Robustness analysis

We now investigate the impact of various image distortions on the verification performance of the tested models.

Noise: The first type of distortion we explore is noise and first look at the impact of additive Gaussian noise. As can be seen from Fig. 3 (top left) the negative effect of Gaussian noise on the selected models verification accuracy is significant. For the MC model the EER score rises proportionally with σ , whereas this is not the case for the WLD and RLT models, where the smallest value of σ already has a detrimental effect on the EER score of the two models. This can also be seen from Figs. 4(a) and 4(b) where the effect of different values of σ on the visual appearance of the feature images of the three models is shown. For the RLT and WLD models the difference in feature images for different σ is not significant - images already look poor for smaller values

of σ and do not change much with an increase in σ . For the MC models, on the other hand, the feature image with less noise retains more of the original vein patterns.

The impact of salt-and-pepper noise on the verification accuracy of the models is almost identical to additive Gaussian noise, as can be observed from Fig. 3 (top right) We again see a detrimental effect for all models, with the WLD and RLT model being particularly sensitive to even small amounts of noise. We also observe a similar effect on the appearance of the feature images in Figs. 4(c) and 4(d) where there is no large difference in feature images for σ values of 30 and 80 for the WLD and RLT models, as opposed to the MC model, where the difference in the vein pattern is very clearly visible. This again suggest that the performance degradation for the MC model is proportional to the amount of noise.

Blur: Next, we explore the impact of Gaussian blur on the verification accuracy of the finger vein models. We see from the results in Fig. 3 (bottom left) that Gaussian blur does not have as negative of an effect on the models verification performance as Gaussian noise. Here, the MC and the RLT models seem to be more robust to blur than the WLD technique as their rate of change in EER score is not as high as for the WLD model. This can also be seen from the feature images in Fig. 4(e) and 4(f), where the vein patterns seem to completely disappear for higher values of σ for the WLD model,

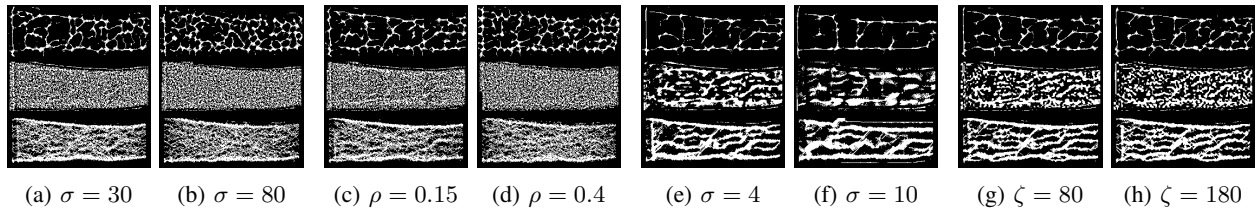


Figure 4.: Impact of different types and levels of noise on feature images of the tested models (from top to bottom): MC, WLD, RLT. a) and b) Gaussian Noise with different values of σ . c) and d) Salt and pepper noise with different values of ρ .

while the features images for the MC and RLT models appear to retain the original vein patterns relatively well even for higher values of σ .

JPEG2000: Finally, we explore the impact of compression artifacts of the performance of the considered finger vein models. It can be seen from Fig. 3 (bottom right) that of all the distortions considered in this work, JPEG2000 compression degrades the performance of the models the least. We observe that the MC and the RLT models are more robust to this type of degradation than the WLD model for higher compression ratios. This can also be seen from Figs. 4(g) and 4(h) from the feature images of the RLT and MC models, which appear identical in their vein patterns for low and high compression ratios (80, 180), while WLD does not retain the vein patterns for higher compression ratios as well as the aforementioned techniques. In comparison to the study of Ablinger *et al.* [6] we observe a similar change in the EER score over the same range of compression ratios.

5 CONCLUSION

We have presented a comprehensive analysis of the effects of different types and levels of image distortion on finger vein recognition. Our main findings are the following:

- Each of the three analysed finger vein models are susceptible to noise and blur distortions by varying degrees, while being mostly robust to JPEG2000 compression artifacts. This indicates that more effort should be put into developing models that are more robust to image degradations, such as noise and blur.
- The analysed models were most easily degraded in performance by Gaussian noise and salt-and-pepper noise, although there is a difference in the rate of performance degradation. Specifically, the WLD and RLT models exhibit substantially higher degradations than MC.
- Gaussian blur was found to significantly negatively effect the verification performance, especially on the WLD model. However, the performance degradation starts at much larger values of σ for the RLT

and MC models.

- JPEG2000 compression had the least affects on the verification accuracy of the finger vein models. The EER scores of all the models considered increased only slightly through the different levels of compression.

None of the analysed models was found to considerably outperform the others in regards to robustness to image degradations, although the WLD model is the least robust overall due to its poor verification performance when subjected to blur and compression artifacts compared to the MC and RLT models.

REFERENCES

- [1] B. Huang, Y. Dai, R. Li, D. Tang, and W. Li, "Finger-vein authentication based on wide line detector and pattern normalization," in *ICPR*, 2010.
- [2] Y. Lu, S. Yoon, S. Wu, and D. S. Park, "Pyramid histogram of double competitive pattern for finger vein recognition," *IEEE Access*, 2018.
- [3] N. Miura, A. Nagasaka, and T. Miyatake, "Extraction of finger-vein patterns using maximum curvature points in image profiles," *TIS*, 2007.
- [4] —, "Feature extraction of finger-vein patterns based on repeated line tracking and its application to personal identification," *MVA*, 2004.
- [5] Y. Zhang, W. Li, L. Zhang, X. Ning, L. Sun, and Y. Lu, "Adaptive learning gabor filter for finger-vein recognition," *IEEE Access*, 2019.
- [6] V. Ablinger, C. Zenz, J. Hämmerle-Uhl, and A. Uhl, "Compression standards in finger vein recognition," in *ICB*, 2016.
- [7] C. Kauba and A. Uhl, "Robustness of finger-vein recognition," in *Hand-Based Biometrics: Methods and technology*, M. Drhansky, Ed., 2018.
- [8] R. Das, E. Piciuccio, E. Maiorana, and P. Campisi, "Convolutional neural network for finger-vein-based biometric identification," *IEEE TIFS*, 2018.
- [9] M. Vanoni, P. Tome, L. El Shafey, and S. Marcel, "Cross-database evaluation with an open finger vein sensor," in *BioMS*, 2014.
- [10] A. Uhl, C. Busch, S. Marcel, and R. Veldhuis, *Handbook of vascular biometrics*. Springer, 2020.
- [11] H. Wang, M. Du, J. Zhou, and L. Tao, "Weber local descriptors with variable curvature gabor filter for finger vein recognition," *IEEE Access*, 2019.
- [12] Z. Xiong, M. Liu, and Q. Guo, "Finger vein recognition method based on center-symmetric local binary pattern," in *ICAICA*, 2019.
- [13] N. Hu, H. Ma, and T. Zhan, "A new finger vein recognition method based on LBP and 2DPCA," in *CCC*, 2018.

- [14] N. M. Kamaruddin and B. A. Rosdi, "A new filter generation method in pcanet for finger vein recognition," *IEEE Access*, 2019.
- [15] H. Hu, W. Kang, Y. Lu, Y. Fang, H. Liu, J. Zhao, and F. Deng, "FV-Net: learning a finger-vein feature representation based on a CNN," in *ICPR*, 2018.
- [16] E. C. Lee, H. C. Lee, and K. R. Park, "Finger vein recognition using minutia-based alignment and local binary pattern-based feature extraction," *IJIST*, 2009.
- [17] K. Grm, V. Štruc, A. Artiges, M. Caron, and H. K. Ekenel, "Strengths and weaknesses of deep learning models for face recognition against image degradations," *IET Biometrics*, vol. 7, no. 1, pp. 81–89, 2017.

Dalibor Maljurič is an MSc student at the Faculty of Electrical Engineering, University of Ljubljana. His thesis research is in the field of anomaly detection. He is also employed at MBVision as a machine vision engineer.

Klemen Grm earned his PhD at the Faculty for Electrical Engineering, University of Ljubljana, in 2020. He is a teaching assistant at the Machine Intelligence Laboratory at the Faculty for Electrical Engineering. His research areas include machine learning, biometrics and image processing.